Supplementary Material: Modelling the impact of the Omicron BA.5 subvariant in New Zealand

Audrey Lustig, Giorgia Vattiato, Oliver Maclaren,
Leighton M. Watson, Samik Datta, Michael J. Plank

Contents

1 Supplementary Methods

1.1 Transmission dynamics

The transmission dynamics are governed by a set of ordinary differential equations for the susceptible (S), exposed (E), clinical infectious (I), subclinical infectious (A) and recovered (R) compartments for each age group $i = 1, \ldots, n_A$ and susceptibility class $k = 1, \ldots, n_S$:

$$\frac{dS_{ik}}{dt} = -\lambda_i(1 - e_{I,k})S_{ik} + W_{ik} + G_{ik} \quad (1)$$

$$\frac{dE_{ik}}{dt} = \lambda_i(1 - e_{I,k})S_{ik} - 1/t_E E_{ik} \quad (2)$$

$$\frac{dI_{ik}}{dt} = 1/t_E p_{\text{clin},i}(1 - e_{S,k})E_{ik} - 1/t_I I_{ik} \quad (3)$$

$$\frac{dA_{ik}}{dt} = 1/t_E \left(1 - p_{\text{clin},i}(1 - e_{S,k})\right) E_{ik} - 1/t_I A_{ik} \quad (4)$$

$$\frac{dR_{ik}}{dt} = 1/t_I(I_{ik} + A_{ik}) - r_w \hat{r} R_{ik}, \quad (5)$$

where t_E and t_I are the latent and infectious periods, respectively, $p_{\text{clin},i}$ is the probability of infection causing clinical symptoms in age group i, r_w is the waning rate, and $\hat{r}$ is the relative rate of moving from recovered (R) to susceptible (S). For each susceptible compartment, there are associated compartments for people who are: exposed but not yet infectious (E); infectious and with clinical symptoms (I); infectious and subclinical (A); recovered and temporarily immune (R). Note that subclinical refers to people who never develop symptoms. For simplicity we do not distinguish between the pre-symptomatic and symptomatic stages of the infectious period for clinical individuals, although it would be straightforward to do this, for example to model symptom-based interventions. Parameter values are shown in Supplementary Tables 1–3. The assumed values for the mean latent and infectious periods represent a mean generation interval of 3.3 days, which is similar to estimates of Abbott et al. (2022); Wu et al. (2022) for the Omicron variant and shorter than that of previous variants of SARS-CoV-2.

The W_{ik} and G_{ik} terms represent waning and vaccination dynamics (see Sec. 1.2). The force of infection λ_i acting on age group i is:

$$\lambda_i = \frac{U R_{EI}(t) u_i}{t_I N_i} \sum_{j=1}^{n_A} M_{ji} \left[\sum_{k=1}^{n_S} (1 - e_{T,k})(I_{jk} + \tau A_{jk}) + t_I n_{\text{seed},j}(t) \right] \quad (6)$$

where $R_{EI}(t)$ is the time-varying reproduction number excluding effects of immunity, N is the total population size in each age group, $n_{\text{seed},j}(t)$ is the number of daily seed infections in age group j at time t, τ is the relative infectiousness of subclinical individuals, u_i is the susceptibility of age group i relative to the 60-64 year age group, and M_{ji} is the average

number of daily contacts in age group i by someone in age group j. The normalising constant U is set to be

$$U = \rho\left[\left(p_{\text{clin},j} + \tau(1 - p_{\text{clin},j})\right) u_i M_{ji}\right]^{-1}$$

where $\rho[.]$ denotes dominant eigenvalue. This normalisation ensures that the reproduction number at time t would be $R_{EI}(t)$ in a fully susceptible population. $R_{EI}(t)$ represents the value the reproduction number would take if there was no immunity in the population, and hence it is unaffected by vaccination, infection and waning dynamics. It therefore provides a way to model time-dependence in contact rates, for example as a result of behavioural change or policy response.

The contact matrix M was allowed to vary over time to model a change in age-structured contact rates (see Methods). The contact matrix at time t was defined as

$$M(t) = (1 - \beta(t))M_0 + \beta(t)M_1 \tag{7}$$

where M_1 is the pre-pandemic contact matrix estimated by Prem et al. (2017) and adjusted for the New Zealand population by Steyn et al. (2022), and M_0 is a modified form of this contact matrix with lower contact rates in older groups and higher contact rates in younger groups (see Vattiato et al., 2022, and Supplementary Figure 1). The time-varying function $\beta(t)$ was defined to be 0 in period 1 (i.e. up to around mid-March 2022 - see Table 1), to increase linearly to α_M over a 50–90 day time window after the end of period 1, and to remain constant at a constant value of α_M subsequently. The value of $\alpha_M \in [0, 1]$ was fitted with the ABC algorithm as described in Methods.

1.2 Vaccination and waning

As indicated above, the G_{ik} term in Eq. (1) represents transitions between susceptible compartments which occur as a result of vaccination (green arrows in Figure 1 of the main text). For the purposes of calculating this, we define five groups of susceptible compartments S^g:

$$\text{0 doses and not previously infected:} \qquad S^g_{i0} = S_{i1} \tag{8}$$

$$\text{1 dose and not previously infected:} \qquad S^g_{i1} = S_{i2} \tag{9}$$

$$\text{2 doses and not previously infected:} \qquad S^g_{i2} = \sum_{k=3}^{6} S_{ik} \tag{10}$$

$$\geq \text{3 doses and not previously infected:} \qquad S^g_{i3} = \sum_{k=7}^{10} S_{ik} \tag{11}$$

$$\text{previously infected:} \qquad S^g_{ip} = \sum_{k=11}^{14} S_{ik} \tag{12}$$

We assumed that all vaccine doses are given to people who are in a susceptible compartment (which is reasonable given the recommendation to wait at least 3 months after testing positive before getting vaccinated).

The total number of people $V_{id}(t)$ in each age group who have received at least d doses of the vaccine at time t is:

$$\frac{dV_{id}}{dt} = v_{id}(t) \tag{13}$$

where $v_{id}(t)$ is the number of d^{th} doses per day given to people in age group i at time t, plus estimated future uptake of fourth doses according to Ministry of Health projections (see Supplementary Figure 2).

We assumed that the v_{id} d^{th} doses ($d = 1, 2, 3$) given to people in age group i at time t are split pro rata between people who have not been previously infected and people who have. This implies that the daily proportion of those not previously infected in age group i receiving their d^{th} dose at time t is

$$p^u_{i,d} = \frac{v_{i,d}}{V_{i,d-1} - V_{i,d}} \tag{14}$$

noting that $V_{i,0} = N_i$, i.e. the total population size in age group i. This accounts for $p^u_{i,d} S^g_{i,d-1}$ of the $v_{i,d}$ doses. The remainder of these doses, $v_{i,d} - p^u_{i,d} S^g_{i,d-1}$, are given to previously infected people. This implies that the daily proportion of those previously infected in age group i receiving their d^{th} dose at time t is

$$p^p_{i,d} = v_{i,d} \frac{V_{i,d-1} - V_{i,d} - S^g_{i,d-1}}{(V_{i,d-1} - V_{i,d}) S^g_{i,p}} \tag{15}$$

The corresponding equations for 4th or subsequent doses are

$$p^u_{i,4+} = \frac{v_{i,4+}}{V_{i,3}} \tag{16}$$

$$p^p_{i,4+} = v_{i,4+} \frac{V_{i,3} - S^g_{i,3}}{V_{i,3} S^g_{i,p}} \tag{17}$$

We may then write the proportion of compartment S_{ik} receiving a vaccine dose per day as:

$$P_{i,k} = \begin{cases} p^u_{i,1}, & \text{if } k = 1 \\ p^u_{i,2}, & \text{if } k = 2 \\ p^u_{i,3}, & \text{if } 3 \leq k \leq 6 \\ p^u_{i,4+}, & \text{if } 7 \leq k \leq 10 \\ \sum_{d=1}^{4+} p^p_{i,d}, & \text{if } 11 \leq k \leq 14 \end{cases} \tag{18}$$

We assumed that receiving a vaccine dose following prior infection has the effect of moving people back to the first post-infection compartment ($S_{i,11}$) and that receiving a 4th dose without any prior infection has the effect of moving people back to the first 3-dose compartment ($S_{i,7}$).

The term G_{ik} appearing in Eq. (1) is now defined as:

$$G_{ik} = \sum_{l=1}^{n_S} P_{il} S_{il} Q^V_{lk} \tag{19}$$

where Q^V_{lk} is the flux into susceptible compartment k from susceptible compartment l as a result of vaccine doses given to people in susceptible compartment l, such that the row sums of the matrix Q^V are all 0.

The term W_{ik} in Eq. (1) represents transitions between susceptible compartments, and transitions from recovered to susceptible compartments, that occur as a result of waning and is defined as:

$$W_{ik} = r_w \left(\sum_{l=1}^{n_S} S_{il} Q^S_{lk} + \hat{r} \sum_{l=1}^{n_S} R_{il} Q^R_{lk} \right) \tag{20}$$

where Q^S_{lk} is the flux into susceptible compartment k from susceptible compartment l (with $Q^S_{kk} \leq 0$ representing the flux out of compartment k) such that the row sums of the matrix Q^S are all 0; and $Q^R_{kl} \geq 0$ is the flux into susceptible compartment k from recovered compartment l such that the row sums of Q^R are all 1.

1.3 Population dynamics

The dynamics of birth, death and ageing are incorporated into the model via additional terms in Eqs. (1)–(13) of the form:

$$\frac{dX_{1,k}}{dt} = b - r_a X_{1,k} - \mu_1 X_{1,k} \tag{21}$$

$$\frac{dX_{i,k}}{dt} = r_a (X_{i-1,k} - X_{i,k}) - \mu_i X_{i,k} \tag{22}$$

$$\frac{dX_{n_A,k}}{dt} = r_a X_{n_A-1,k} - \mu_{n_A} X_{n_A,k} \tag{23}$$

where b is the birth rate per unit time, r_a is ageing rate per unit time (equal to the reciprocal of the size of the age bands, in this case 5 years) and μ_i is the per capita death rate per unit time in age group i. Here X may be any one of the infection states (S, E, I, A, R) or V. For simplicity we assume that the the aggregate population death rate is independent of the transmission dynamics.

The total number of annual births and the annual death rate in 5-year age bands up to age 75 were taken from StatsNZ data for 2019 (StatsNZ, 2022). The annual death rate for the over-75-years age group was set to give a similar equilibrium age distribution to the StatsNZ 2022 estimated resident population (StatsNZ, 2022).

Parameter	Value	Source
Epidemiological parameters		
Latent period	$t_E = 1$ day	Wu et al. (2022)
Infectious period	$t_I = 2.3$ days	Abbott et al. (2022)
Mean time from onset of infectiousness to positive test result	$t_T = 4$ days	Vattiato et al. (2022)
Mean time from test result to hospital admission	$t_H = 1$ days	Assumed
Mean time from admission to death	$t_F = 14$ days	Assumed
Relative infectiousness of subclinical individuals	$\tau = 0.5$	Davies et al. (2020)
Probability of testing (clinical)	$p_{\text{test,clin}} \sim U[0.35, 0.75]$	Fitted
Probability of testing (sublinical)	$p_{\text{test,sub}} = 0.4 p_{\text{test,clin}}$	Assumed
Date-specific parameters		
Date of seeding with infectious cases	19 Jan 2022 $+U[-3, 3]$	Fitted
Number of seed cases in age group i	$0.0001 N_i$	Assumed
$R_{EI}(t)$ in period 1	$R_{EI,1} \sim U[2.0, 2.4]$	Fitted
$R_{EI}(t)$ in period 2	$R_{EI,2} \sim U[2.9, 4.9]$	Fitted
End of period 1	10 Mar 2022 $+U[-5, 5]$)	Fitted
Period 1 – period 2 ramp window	$U[35, 75]$ days	Fitted
Relaxation of contact matrix	$\alpha_M \sim U[0, 0.8]$	Fitted
Contact matrix ramp window	$U[50, 90]$ days	Fitted
Variant model		
BA.5 immune escape [low,baseline,high]	$r_{VOC} = [0.19, 0.39, 0.59]$	Manually tuned
BA.5 change in vaccine-derived log antibody titre relative to BA.2	$\Delta n_{0,VOC} = -0.92$	Khan et al. (2022) Hachmann et al. (2022)
BA.5 dominance date	$t_{VOC} = 20$ Jun 2022	Manually tuned
Variant transition window	$\sigma_{VOC} = 2$ days	Assumed

Table 1: Model parameter values and prior distributions.

Age (yrs)	Popn $N_i(0)$	u_i	$p_{\text{clin},i}$	IHR_i per 1000	IFR_i per 1000	$t_{LOS,i}$ (days)	μ_i (per 1000 per yr)
0-4	305055	0.46	54%	0.94	0.0034	2.0	1.07
5-9	327520	0.46	55%	0.94	0.0034	2.0	0.08
10-14	336975	0.45	58%	0.40	0.0034	2.0	0.17
15-19	316980	0.56	60%	0.60	0.0062	2.0	0.41
20-24	329695	0.79	62%	0.87	0.012	2.0	0.60
25-29	370120	0.93	64%	1.25	0.024	2.0	0.56
30-34	379010	0.97	66%	1.84	0.048	2.7	0.73
35-39	340755	0.98	68%	2.69	0.091	3.3	0.83
40-44	312245	0.94	70%	3.81	0.180	4.0	1.21
45-49	325050	0.93	71%	5.61	0.360	4.7	1.95
50-54	333210	0.94	73%	8.32	0.697	5.4	3.07
55-59	325780	0.97	74%	11.7	1.35	6.0	4.45
60-64	298820	1.00	76%	16.9	2.65	6.7	6.49
65-69	254865	0.98	77%	23.8	5.08	7.4	10.27
70-74	220245	0.90	78%	33.3	9.74	8.0	16.69
75+	346280	0.86	80%	59.7	54.7	8.7	136.0

Table 2: Age-dependent model parameters: 'Popn' is the initial population size in each age group; u_i is the susceptibility of age group i relative to the 60-64 year age group; $p_{clin,i}$, IHR_i and IFR_i are respectively the proportion of infections causing clinical disease, hospitalisation and death respectively for individuals with no immunity (i.e. unvaccinated and no prior infection); $t_{LOS,i}$ is the average length of hospital stay estimated from MOH data on duration of patients receiving hospital treatment for Covid-19; μ_i is the all-cause death rate per 1000 people per year. Values of $p_{clin,i}$ are from Hinch et al. (2021). The age-dependence in IHR_i and IFR_i is based on the results of Herrera-Esposito and de Los Campos (2022) but are scaled down for consistency with New Zealand's observed hospitalisation and death rates, reflecting a combination of the virulence of Omicron relative to earlier variants and tightening definitions to exclude incidental hospitalisations and deaths. The values of IFR_i the Table are multiplied by a factor $\alpha_{\text{IFR}} \sim U[0.5, 1.5]$ and the values of IHR_i are multiplied by a factor $\alpha_{\text{IHR}} \sim U[0.5, 1.5]$. Total birth rate $b = 59637$ yr^{-1}.

1.4 Immunity model

We assume immunity for people who are transiently in the one-dose compartment is negligible. Hence $e_{O1} = e_{O2} = 0$ for all outcomes O. We set the log antibody titre for susceptible compartments $k = 3$ and $k = 7$ equal to the estimates of Golding and Lydeamore (2022) for the initial log neutralising titre for 2 doses $n_{2d,0}$ and 3 doses $n_{3d,0}$ respectively of the Pfizer/BioNTech BNT162b2 vaccine against Omicron (see Supplementary Table 3).

Following recovery from a first infection, people who have had 3 doses of the vaccine (i.e. those in recovered compartments $k = 7, \ldots, 10$) all move initially to susceptible compartment $k = 11$. This is encoded by the matrix Q^R in Supplementary sec. 1.2: $Q^R_{k,11} = 1$ for $k = 7, \ldots 10$.

Following recovery from a first infection, fixed proportions of those in recovered compartments $k = 3, \ldots, 6$ (2 vaccine doses) move to the lower-immunity compartments $k = 12, 13, 14$. To determine what these proportions should be we note that, absent any subsequent immunising events, the proportion $q_k(t)$ of a cohort of individuals that entered susceptible compartment $k = 11$ at time $t = 0$ that is in compartment k at time t satisfies

$$\dot{q}_k = \begin{cases} -r_w q_k, & k = 11, \\ r_w(q_{k-1} - q_k), & k = 12, 13, \\ r_w q_{k-1}, & k = 14, \end{cases} \tag{24}$$

where $q_{11}(0) = 1$ and $q_k(0) = 0$ for $k = 12, 13, 14$. The average log antibody titre of the cohort at time t is $\bar{n}(t) = \sum_k n_k q_k(t)$. We set $Q^R_{kl} = q_l(t^*)$ where t^* is such that $\bar{n}(t^*) - \bar{n}(0) = n_{p2d,0} - n_{p3d,0}$, the estimated difference in initial log titre between prior infection plus 2 doses and prior infection plus 3 doses according to Golding and Lydeamore (2022).

A similar approach is applied to those moving out of recovered compartments $k = 1, 2$ (i.e. people with 0 or 1 vaccine doses following recovery from a first infection): we set $Q^R_{kl} = q_l(t^*)$ where t^* is such that $\bar{n}(t^*) - \bar{n}(0) = n_{p,0} - n_{p3d,0}$. Following recovery from a second or subsequent infection, everyone moves initially to susceptible compartment $k = 11$ regardless of vaccination status: $Q^R_{k,11} = 1$ for $k = 11, \ldots, 14$.

To implement the assumptions for an immune escape variant (see Methods), we applied a time-limited increase in the magnitude of the waning fluxes in Eq. (20) for the post-infection compartments:

$$W_{ik} = \left(r_w + r_{VOC}\phi\left(\frac{t - t_{VOC}}{\sigma_{VOC}}\right)\right)\left(\sum_{l=1}^{n_S} S_{il} Q^S_{lk} + \hat{r}\sum_{l=1}^{n_S} R_{il} Q^R_{lk}\right), \qquad k = 11, 12, 13, 14 \tag{25}$$

where $\phi(.)$ is the standard normal probability density function. This formulation means that movement of people to a lower post-infection immunity compartment takes place at

Parameter	Value	Source
Initial log antibody titre:		
- 2 doses	$n_{2d,0} = -1.61$	Golding and Lydeamore (2022)
- 3 doses	$n_{3d,0} = -0.92$	Golding and Lydeamore (2022)
- prior infection with 0/1 doses	$n_{p,0} = 1.39$	Manually tuned
- prior infection with 2 doses	$n_{p2d,0} = 2.71$	Manually tuned
- prior infection with 3 doses	$n_{p3d,0} = 3.56$	Manually tuned
Log antibody titre providing 50% immunity:		
- against infection	$n_{\text{inf},50} = -1.61$	Khoury et al. (2021)
- against hospitalisation	$n_{\text{hosp},50} = -3.51$	Khoury et al. (2021)
- against death	$n_{\text{death},50} = -3.51$	Khoury et al. (2021)
Waning rate	$r_w \sim U[0.0027, 0.0063]$ day^{-1}	Fitted
Relative rate of moving from R to S	$\hat{r} = 1.85$	Assumed
Drop in log titre in subsequent compartment	$n_{\text{drop}} = 2.30$	Assumed
Slope of logistic function	$\kappa = 1.28$	Khoury et al. (2021)
Minimum long-term immunity to hospitalisation and death	$e_{\text{sev,min}} = 0.5$	Assumed

Table 3: Parameters for the immunity submodel. All log titres are given as natural logarithms and represent neutralisation of BA.2. The drop in neutralising titre for BA.5 relative to BA.2 is as described in Methods.

$t = t_{VOC}$ in a short time window of duration determined by the parameter σ_{VOC}. In the limit $\sigma_{VOC} \to 0$, this movement occurs as an instantaneous pulse; larger values of σ correspond to a more gradual change. We chose an arbitrary value of $\sigma_{VOC} = 2$ days, representing a relatively rapid takeover of BA.5 from BA.2; larger values of σ_{VOC} would result in a more gradual change in the epidemic growth rate at the start of the BA.5 wave.

1.5 Clinical pathways and fitting to data

The process of testing and progress to different clinical endpoints (hospital admission, hospital discharge, and death) can be modelled downstream of the transmission dynamics. We model the number of newly infectious people in each age group who will eventually become

a confirmed case (C), be hospitalised (H), and die (F) via the differential equations.

$$\frac{dC_{i1}}{dt} = 1/t_E \sum_{k=1}^{n_S} \left(p_{\text{test,clin}} p_{\text{clin},i} \frac{1-e_{S,k}}{1-e_{I,k}} + p_{\text{test,sub}} \left(1 - p_{\text{clin},i} \frac{1-e_{S,k}}{1-e_{I,k}} \right) \right) E_{ik} - \alpha_1 C_{i1} \quad (26)$$

$$\frac{dH_{i1}}{dt} = 1/t_E \text{IHR}_i \sum_{k=1}^{n_S} \frac{1-e_{H,k}}{1-e_{I,k}} E_{ik} - \alpha_1 H_{i1} \quad (27)$$

$$\frac{dF_{i1}}{dt} = 1/t_E \text{IFR}_i \sum_{k=1}^{n_S} \frac{1-e_{F,k}}{1-e_{I,k}} E_{ik} - \alpha_1 F_{i1} \quad (28)$$

$$(29)$$

where IHR_i and IFR_i are respectively the infection hospitalisation ratio and the infection fatality ratio for immune naive individuals in age group i (see Table 2).

The time lag from onset of infectiousness to each endpoint is modelled via transition through a series of compartments:

$$\begin{array}{lll} \frac{dC_{i,2}}{dt} = \alpha_1 C_{i1} - \alpha_2 C_{i2}, & \frac{dH_{i,2}}{dt} = \alpha_1 H_{i1} - \alpha_2 H_{i2}, & \frac{dF_{i,2}}{dt} = \alpha_1 F_{i1} - \alpha_2 F_{i2}, \\ \frac{dC_{i,3}}{dt} = \alpha_2 C_{i2}, & \frac{dH_{i,3}}{dt} = \alpha_2 H_{i2} - \alpha_3 H_{i3}, & \frac{dF_{i,3}}{dt} = \alpha_2 F_{i2} - \alpha_3 F_{i3}, \\ & \frac{dH_{i,4}}{dt} = \alpha_3 H_{i3} - \alpha_{4,i} H_{i4}, & \frac{dF_{i,4}}{dt} = \alpha_3 F_{i3} - \alpha'_4 F_{i4}, \\ & \frac{dH_{i,5}}{dt} = \alpha_{4,i} H_{i4}, & \frac{dF_{i,5}}{dt} = \alpha'_4 F_{i4} - \alpha_5 F_{i5}, \\ & & \frac{dF_{i,6}}{dt} = \alpha_5 F_{i5}. \end{array} \quad (30)$$

where α_k are a set of rate constants determining the time lags. We set $\alpha_1 = \alpha_2 = 2/t_T$ where t_T is the mean time from onset of infectiousness to return of a positive test result. The mean time from positive test result to hospital admission is $t_H = \alpha_3^{-1}$, and the mean length of hospital stay for non-fatal cases in age group i is $t_{LOS,i} = \alpha_{4,i}^{-1}$. We set $\alpha'_4 = \alpha_5 = 2/t_F$ where t_F is the mean time from hospital admission to death.

The compartment C_{i3} represents the observed cumulative number of cases, H_{i4} the number of cases currently in hospital, H_{i5} the cumulative number of hospital discharges and F_{i6} the cumulative number of fatalities in age group i at time t. The other C, H and F variables above represent latent (unobservable) states.

The variables in Eqs. (30) were used to define a number of key model outputs for model fitting and/or comparison with data:

1. New cases per day: $\alpha_2 \sum_i C_{i2}(t)$.
2. Proportion of new cases in over 60s: $\sum_{i \geq 13} C_{i2}(t) / \sum_i C_{i2}(t)$.
3. New admissions per day: $\alpha_3 \sum_i H_{i3}(t)$.
4. New deaths per day: $\alpha_5 \sum_i F_{i5}(t)$.

5. New infections per day: $1/t_E \sum_{i,k} E_{ik}(t)/N_i(t)$.

6. Hopsital occupancy: $\sum_i H_{i4}(t)$

Outputs (1) and (2) were fitted to data from the Ministry of Health on new daily Covid-19 cases reported from 1 March to 7 July 2022, smoothed using a 7-day rolling average. The start date of 1 March was chosen to avoid using data from a period at the start of the first Omicron wave when case ascertainment was likely significantly lower due to a lack of testing availability.

Output (3) was fitted to new daily hospital admissions for Covid-19 from 1 February to 28 May 2022, smoothed using a 7-day rolling average. The chosen end date ignores the most recent 40 days of data to allow for reporting lags. Only hospital admissions categorised by the Ministry of Health as "Covid-related hospitalisation" were included – this is significantly fewer than the totals reported in the daily updates from the Ministry of Health which include all Covid-positive hospital admissions.

Output (4) was fitted to daily Covid-19 deaths 1 February to 27 June 2022, smoothed using a 7-day rolling average. The chosen end date ignores the most recent 10 days of data to allow for reporting lags. Deaths were defined to be cases that were recording as having died and where the cause-of-death summary was "COVID as underlying" ($n = 632$), "COVID as contributory" ($n = 355$), or "Not available" ($n = 141$) were included; deaths where the cause-of-death summary was "Not COVID" ($n = 332$) were excluded.

Output (5) was fitted to data on the weekly incidence of new cases in a routinely tested cohort of approximately 20,000 border workers from 13 February to 3 July 2022. This may not be a representative sample of the population but we include it because, unlike outputs (1–4), it provides longitudinal surveillance data that is less sensitive to either case ascertainment levels or disease severity.

We did not fit to output (6) but we compare model output to data on hospital occupancy as a key measure of load on the healthcare system. To quantify the number of hospital inpatients receiving treatment related to Covid-19 at a given time, we use the hospital admission date, t_a, and the Ministry of Health field for the length of hospital stay that is Covid-related, t_h. We use this field to assign each hospitalised case a pseudo-discharge date $t_d = t_a + t_h$. Hospital occupancy at time t is then defined to be the number of cases with an admission date $t_a \leq t$ and a pseudo-discharge date $t_d > t$. This assumes that each inpatient's period of receiving Covid-related treatment is at the start of their hospital stay, which may not always be true, but is not expected to have a major effect on results.

For each fitted time series (1)–(5), we defined the error function as

$$d(x, y) = 1/n \sum_{t=1}^{n} \left(\ln(x_t + \epsilon) - \ln(y_t + \epsilon)\right)^2, \tag{31}$$

where ϵ is a fixed value that is small relative to typical values of the variable being fitted: we set $\epsilon = 10$ per day for cases, $\epsilon = 0.5$ for hospital occupancy, $\epsilon = 0.01$ per day for deaths, $\epsilon = 5 \times 10^{-5}$ for age distribution of cases, and $\epsilon = 5 \times 10^{-6}$ per day for incidence per capita.

The total error is defined as the sum of the error for outputs (1)–(5). To implement ABC rejection, we solved the model for $N = 50000$ parameter combinations drawn randomly from the prior and retained the 500 simulations with the smallest error. We report the pointwide median and 5th, 25th, 75th and 95th percentiles for each model output across the 500 retained simulations.

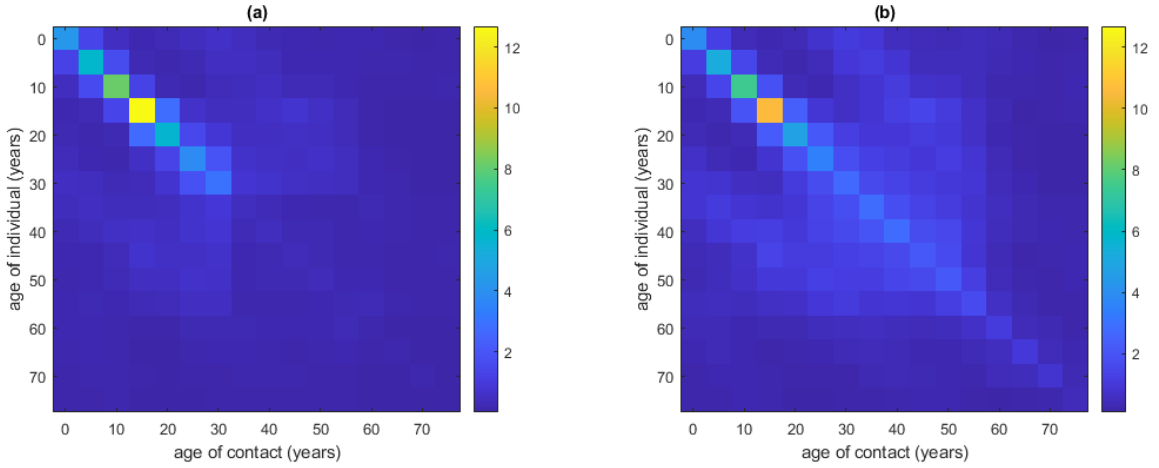

Supplementary Figure 1: Contact matrices showing the average number of contacts between age groups: (a) during period 1 of the simulation (M_0); (b) during period 2 of the simulation (M_1).

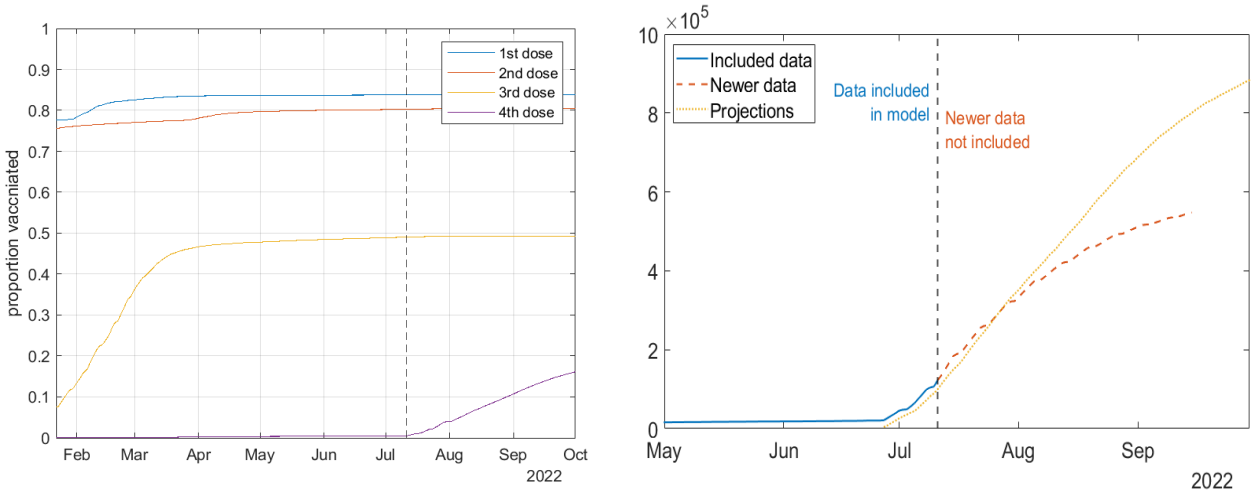

(a) (b)

Supplementary Figure 2: (a) Cumulative number of 1st, 2nd, 3rd and 4th doses of the vaccine relative to New Zealand's population size, based on actual doses administered up to 11 July 2022 (dashed vertical line) and Ministry of Health projections of future uptake of 4th doses after 11 July 2022. (b) Comparison of the Ministry of Health projections of future uptake of 4th doses after 11 July 2022 (yellow curve) with the actual number of 4th doses administered (orange) after 11 July 2022. Note the data for the actual number of 4th doses administered (orange) after 11 July 2022 was not available at the time of the analysis.

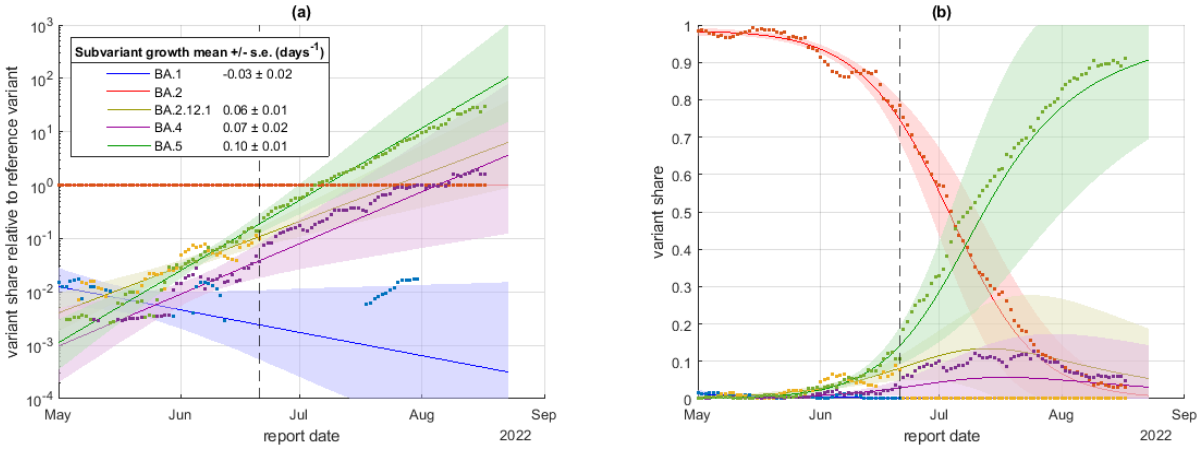

Supplementary Figure 3: Proportion of sequenced community cases that were categorised by ESR (2022) as BA.1, BA.2, BA.2.12.1, BA.4 and BA.5 (points) together with a multinomial regression model (mean and 95% confidence intervals). The model was fitted to data on cases reported up to 21 June 2022 (dashed vertical line), and provides a good prediction of subsequent data. Panel (a) shows the share of each subvariant relative to BA.2, which was the previously dominant variant; (b) shows the absolute share of each subvariant. The multinomial model is equivalent to exponential growth or decay in the ratio of each variant relative to BA.2, which corresponds to straight lines in panel (a). Legend shows the growth rate for each subvariant relative to BA.2 (mean ± standard error of the estimated multinomial coefficient). Note: no data is shown for BA.2.12.1 after 21 June 2022 because ESR subsequently stopped reporting the number of BA.2.12.1 sequences.

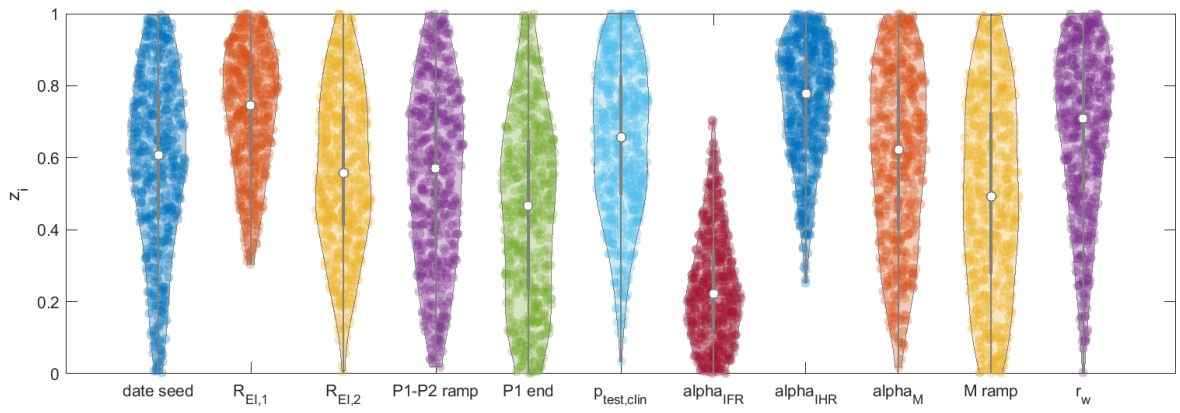

Supplementary Figure 4: Violin plots showing the distribution of each fitted parameter across the 500 accepted realisations of the model with the best fit to the data out of 50,000 random draws from the prior. Each parameter θ_i has a uniform prior $\theta_i \sim U[a_i, b_i]$ (see Tables 1–3) and for the purposes of plotting, each parameter is transformed to the $[0, 1]$ scale via $z_i = (\theta_i - a_i)/(b_i - a_i)$.

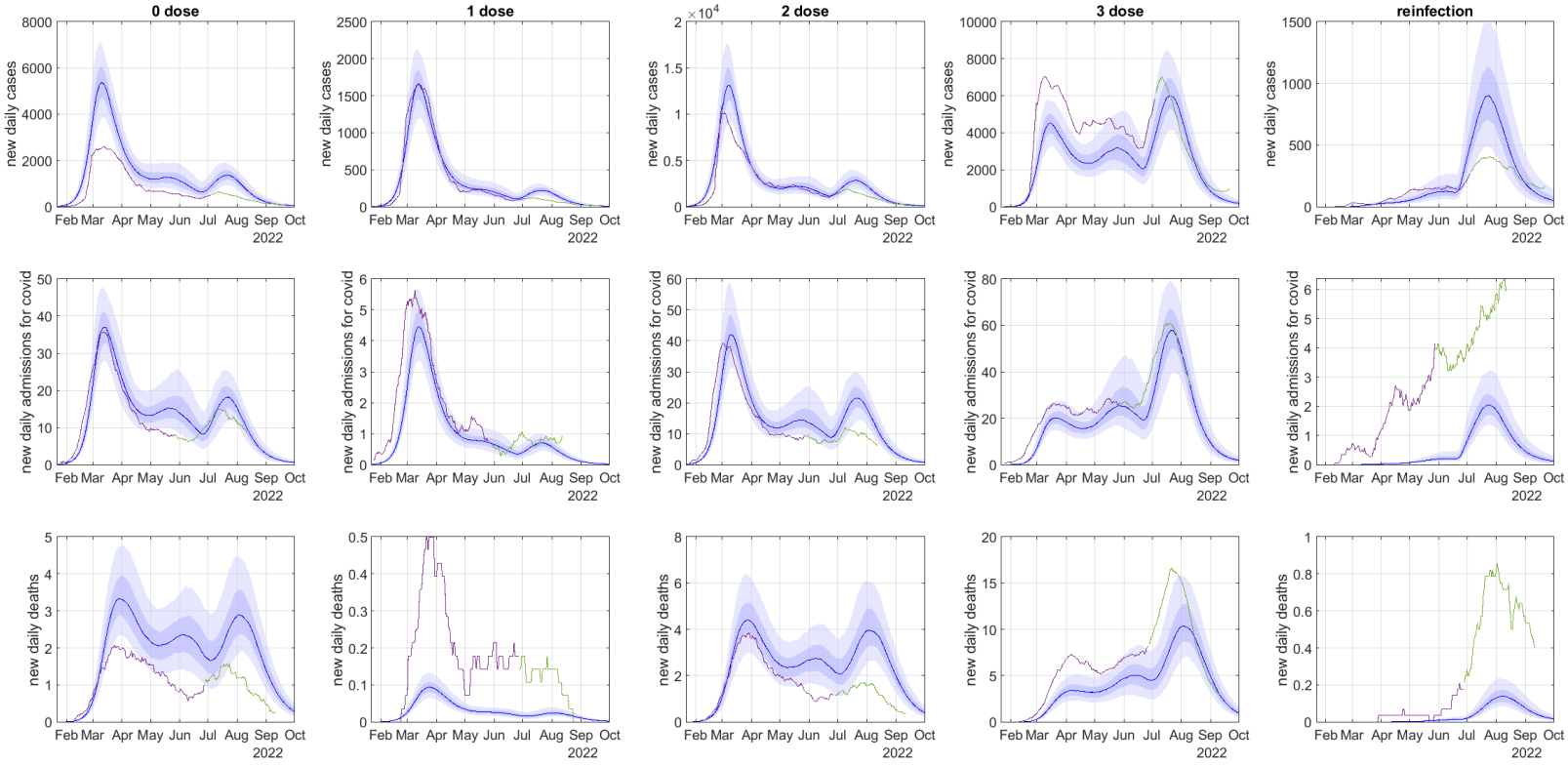

Supplementary Figure 5: Results stratified by immunity status (no prior infections and 0 doses, no prior infections and 1 dose, no prior infections and 2 doses, no prior infection and at least 3 doses, and with prior infection) for the baseline scenario showing new daily cases, new daily hospital admissions and daily deaths. Data on reinfections show individuals with a positive test result reported at least 28 days after a previous positive test results; this definition may include some chronic infections. Model results for reinfections are adjusted for under-ascertainment of the first infection according to the age-specific case ascertainment ratio in the model. Note this assumes that reporting of first infection and subsequent reinfections occur with independently with the same probability, so the comparison should be viewed as approximate. Blue curve shows the median of 500 model simulations and shaded bands show the 5th, 25th, 75th and 95th percentiles. Data (purple curves) show the rolling average over 7 days for cases, 14 days for admissions and 28 days for deaths.

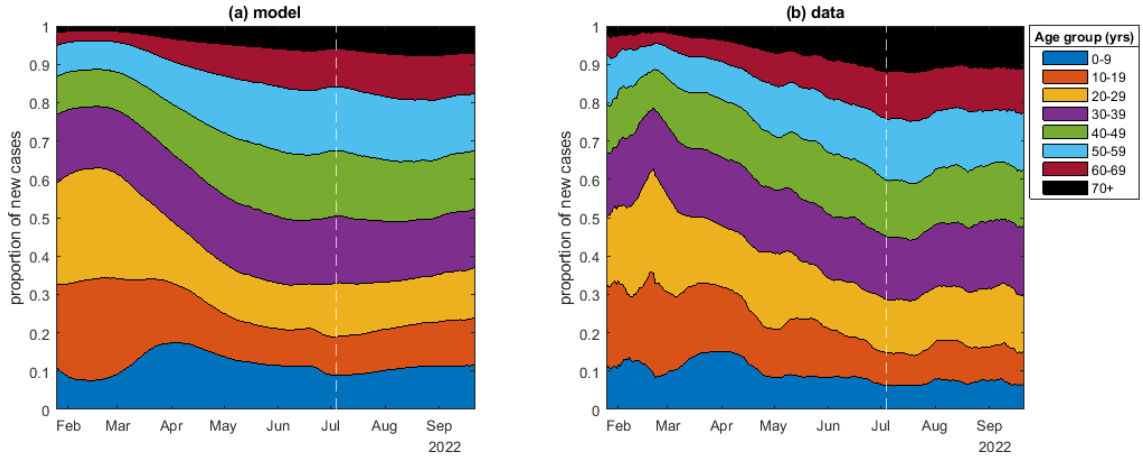

Supplementary Figure 6: Age distribution of new cases in the model compared to the data, shown as the 7-day rolling average. Data before the vertical dotted line at 7 July 2022 was used to fit the model while data afterwards was used for validation.

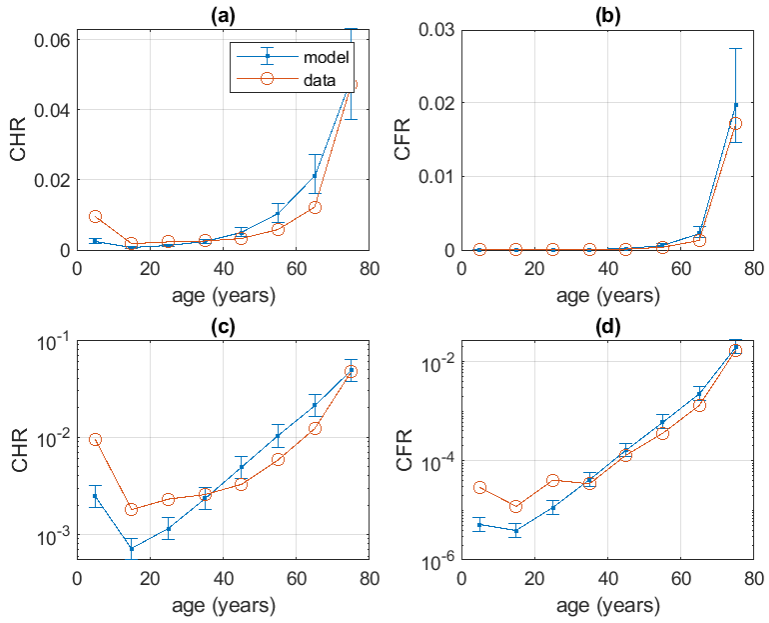

Supplementary Figure 7: Age-specific case hospitalisation ratio (CHR) and case fatality ratio (CFR). Upper plots show results on a linear scale; lower plots show results on a log scale.

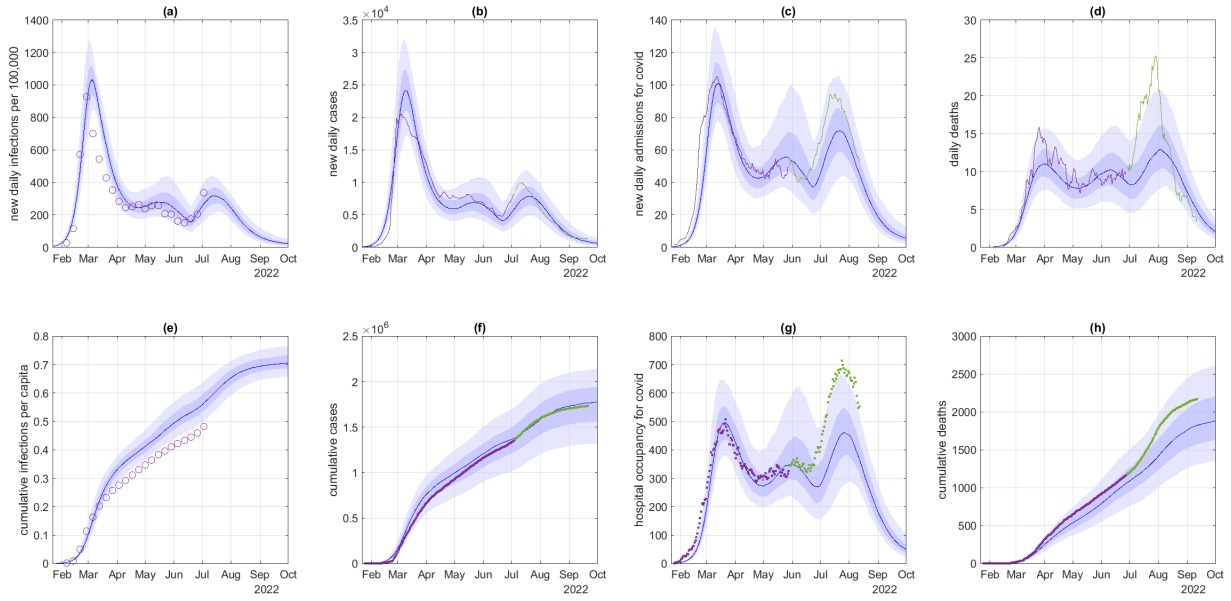

Supplementary Figure 8: As for Figure 3 in the main article but with a smaller growth advantage for BA.5 relative to BA.2 (0.07 day^{-1} instead of 0.09 day^{-1}).

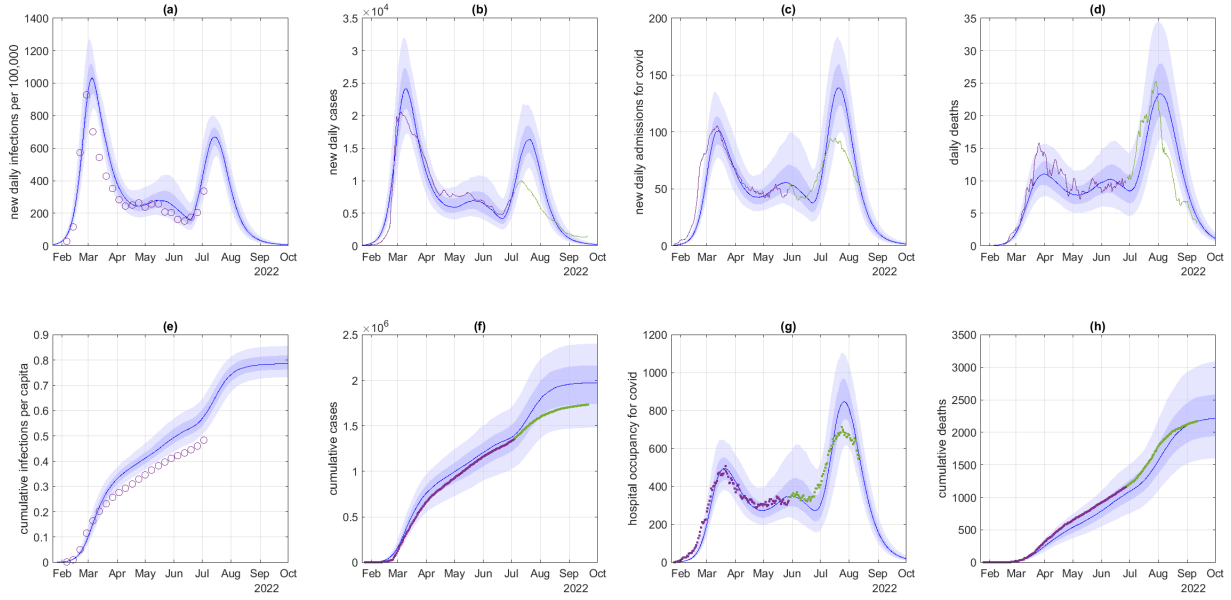

Supplementary Figure 9: As for Figure 3 in the main article but with a larger growth advantage for BA.5 relative to BA.2 (0.12 day^{-1} instead of 0.09 day^{-1}).

References

Abbott, S., Sherratt, K., Gerstung, M., and Funk, S. (2022). Estimation of the test to test distribution as a proxy for generation interval distribution for the Omicron variant in England. *medRxiv*, https://doi.org/10.1101/2022.01.08.22268920.

Davies, N. G., Klepac, P., Liu, Y., Prem, K., Jit, M., and Eggo, R. M. (2020). Age-dependent effects in the transmission and control of covid-19 epidemics. *Nature Medicine*, 26(8):1205–1211.

ESR (2022). Prevelence of SARS-CoV-2 variants of concern in Aoteoroa New Zealand. https://github.com/ESR-NZ/nz-sars-cov2-variants.

Golding, N. and Lydeamore, M. (2022). Analyses to predict the efficacy and waning of vaccines and previous infection against transmission and clinical outcomes of SARS-CoV-2 variants. https://github.com/goldingn/neuts2efficacy. Accessed 5 April 2022.

Hachmann, N. P., Miller, J., Collier, A.-r. Y., Ventura, J. D., Yu, J., Rowe, M., Bondzie, E. A., Powers, O., Surve, N., Hall, K., et al. (2022). Neutralization escape by SARS-CoV-2 Omicron subvariants BA.2.12.1, BA.4, and BA.5. *New England Journal of Medicine*, 387:86–88.

Herrera-Esposito, D. and de Los Campos, G. (2022). Age-specific rate of severe and critical SARS-CoV-2 infections estimated with multi-country seroprevalence studies. *BMC Infectious Diseases*, 22(1):1–14.

Hinch, R., Probert, W. J., Nurtay, A., Kendall, M., Wymant, C., Hall, M., Lythgoe, K., Bulas Cruz, A., Zhao, L., Stewart, A., et al. (2021). OpenABM-Covid19 – An agent-based model for non-pharmaceutical interventions against COVID-19 including contact tracing. *PLoS Computational Biology*, 17(7):e1009146.

Khan, K., Karim, F., Ganga, Y., Bernstein, M., Jule, Z., Reedoy, K., Cele, S., Lustig, G., Amoako, D., Wolter, N., et al. (2022). Omicron BA.4/BA.5 escape neutralizing immunity elicited by BA.1 infection. *Nature Communications*, 13(1):1–7.

Khoury, D. S., Cromer, D., Reynaldi, A., Schlub, T. E., Wheatley, A. K., Juno, J. A., Subbarao, K., Kent, S. J., Triccas, J. A., and Davenport, M. P. (2021). Neutralizing antibody levels are highly predictive of immune protection from symptomatic SARS-CoV-2 infection. *Nature Medicine*, 27(7):1205–1211.

Prem, K., Cook, A. R., and Jit, M. (2017). Projecting social contact matrices in 152 countries using contact surveys and demographic data. *PLoS Computational Biology*, 13(9):e1005697.

StatsNZ (2022). Infoshare. https://infoshare.stats.govt.nz. Accessed 29 May 2022.

Steyn, N., Plank, M. J., Binny, R. N., Hendy, S. C., Lustig, A., and Ridings, K. (2022). A COVID-19 vaccination model for Aotearoa New Zealand. *Scientific Reports*, 12(1):1–11.

Vattiato, G., Maclaren, O., Lustig, A., Binny, R. N., Hendy, S. C., and Plank, M. J. (2022). An assessment of the potential impact of the Omicron variant of SARS-CoV-2 in Aotearoa New Zealand. *Infectious Disease Modelling*, 7:94–105.

Wu, Y., Kang, L., Guo, Z., Liu, J., Liu, M., and Liang, W. (2022). Incubation period of COVID-19 caused by unique SARS-CoV-2 strains: a systematic review and meta-analysis. *Journal of the American Medical Association Network Open*, 5(8):e2228008–e2228008.